

## Supporting Information

### **Constructing Amorphous Lattice Buffering Layers Enable Stable P2-Type Layered Oxide Cathodes for Sodium-Ion Batteries**

Yuanye Wutian,<sup>b†</sup> Yang Wang,<sup>a†</sup> Kaiyu Liu,<sup>a</sup> Weifang Liu,<sup>\*c</sup> Chen Tao<sup>\*a</sup>

## **Experimental Procedure**

### **Synthesis of NMNF, NMN and NMF**

NMNF, NMN, and NMF materials were synthesized via a solid-state ball-milling method. Taking NMNF as an example, anhydrous sodium carbonate ( $\text{Na}_2\text{CO}_3$ , Sinopharm), manganese (III) oxide ( $\text{Mn}_2\text{O}_3$ ), nickel oxide ( $\text{NiO}$ ), and iron (III) oxide ( $\text{Fe}_2\text{O}_3$ ) were thoroughly mixed in a mortar according to the corresponding stoichiometric ratios. The resulting mixture was then ball-milled at 400 rpm for 5 hours with a ball-to-powder mass ratio of 20:1. After ball milling, the mixture was scraped from the milling jar using a small spatula and further ground in a mortar. The powder was subsequently calcined in a muffle furnace by heating to 900 °C at a rate of 5 °C  $\text{min}^{-1}$  and holding for 9 hours. After the heating program was completed, the product was rapidly cooled to room temperature at a cooling rate of approximately 10 °C/min. Finally, the product was collected and ground again in a mortar to obtain the final NMNF material. The NMN and NMF samples were prepared using the same procedure.

### **Characterization**

X-ray diffraction (XRD) patterns were recorded on an Ultima IV diffractometer using  $\text{Cu K}\alpha$  radiation over a  $2\theta$  range of 10–80° at a scanning rate of 10°  $\text{min}^{-1}$ . The metal contents of the samples were determined by inductively coupled plasma atomic emission spectroscopy (ICP-AES) using a PerkinElmer 8300 system. Scanning electron microscopy (SEM, JEOL JSM-7610FPlus) and transmission electron microscopy (TEM, Talos F200 and 2100F) were employed to examine the morphology of the materials. High-resolution TEM (HRTEM) images were collected on a Titan G2 electron microscope. X-ray photoelectron spectroscopy (XPS) was conducted using an EscaLab Xi+ system to analyze the elemental binding energies.

### **Electrochemical Measurements**

The cathode electrodes were prepared by thoroughly mixing the active material, acetylene black, and polyvinylidene fluoride (PVDF) in a mass ratio of 8:1:1. N-Methyl-2-pyrrolidone (NMP) was then added as a solvent, and the mixture was ground to form a uniform slurry. The slurry was coated onto aluminum foil and dried in a convection oven at 60 °C for 6 hours,

followed by further drying in a vacuum oven at 80 °C for 12 hours to obtain the cathode electrodes, with an active material loading of approximately 2 mg cm<sup>-2</sup>. CR2016 coin cells were assembled in an argon-filled glovebox, using metallic sodium foil as the anode, a glass fiber membrane (GF/A, Whatman) as the separator, and 1.0 M NaClO<sub>4</sub> dissolved in ethylene carbonate (EC) and diethyl carbonate (DEC) (1:1 v/v) with 5 vol% fluoroethylene carbonate (FEC) as the electrolyte. The electrochemical performance of the electrodes was evaluated in the voltage range of 2.0–4.0 V using a NEWARE battery testing system. Cyclic voltammetry (CV) and electrochemical impedance spectroscopy (EIS) measurements were carried out on a CHI660a electrochemical workstation.

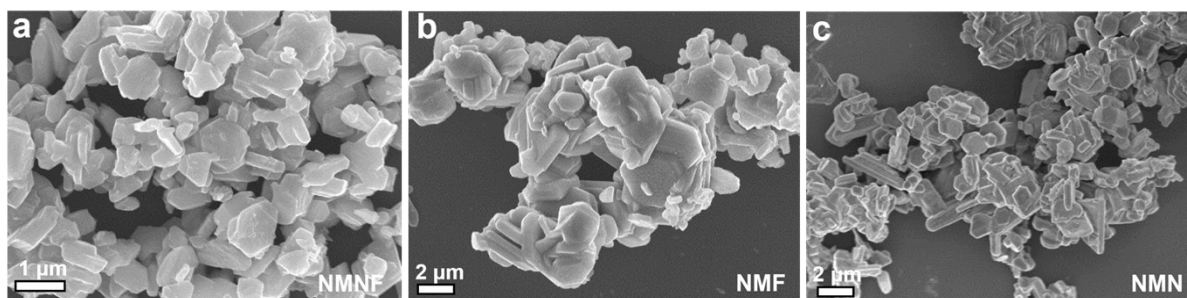


Figure S1. SEM images of (a) NMNF, (b)NMF and (c) NMN.

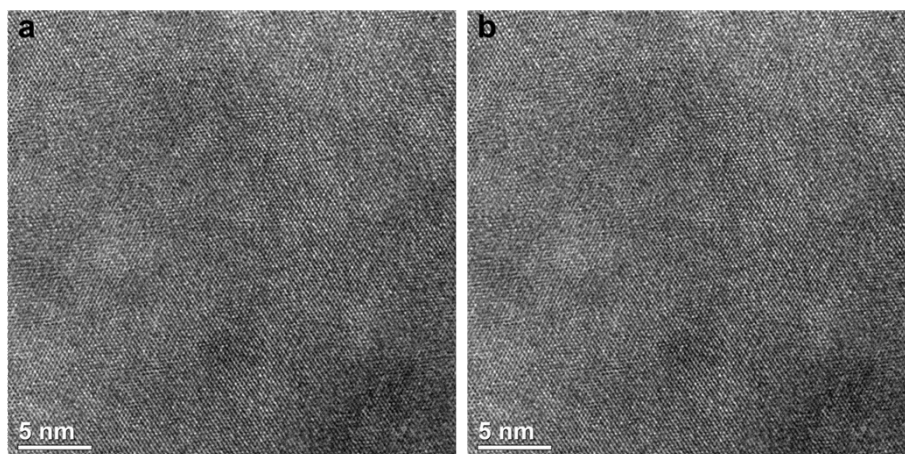


Figure S2. HRTEM images of (a) NMF and (b) NMN.

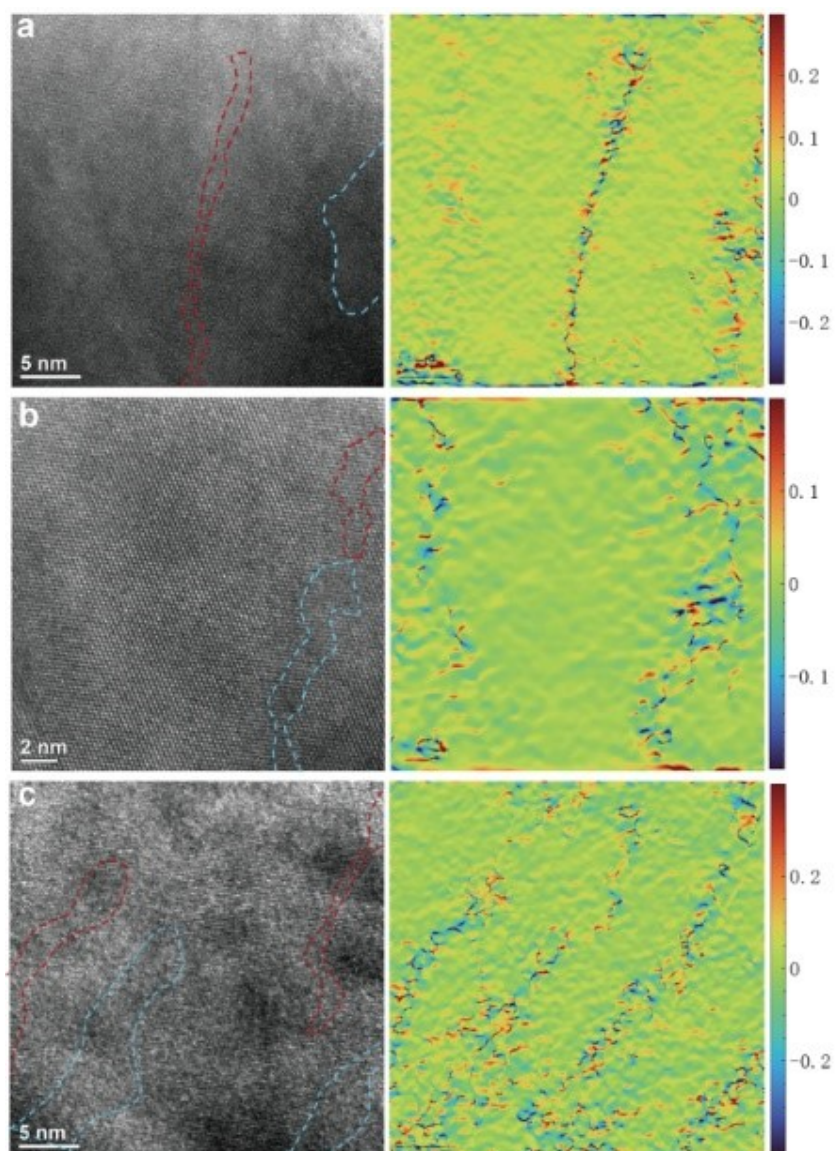


Figure S3. HRTEM images of NMNF and corresponding  $\epsilon_{xx}$  strain distribution maps based on geometric phase analysis. (a, b) TEM images acquired with an exposure time of 3 s; (c) TEM image acquired with an exposure time of 6 s.

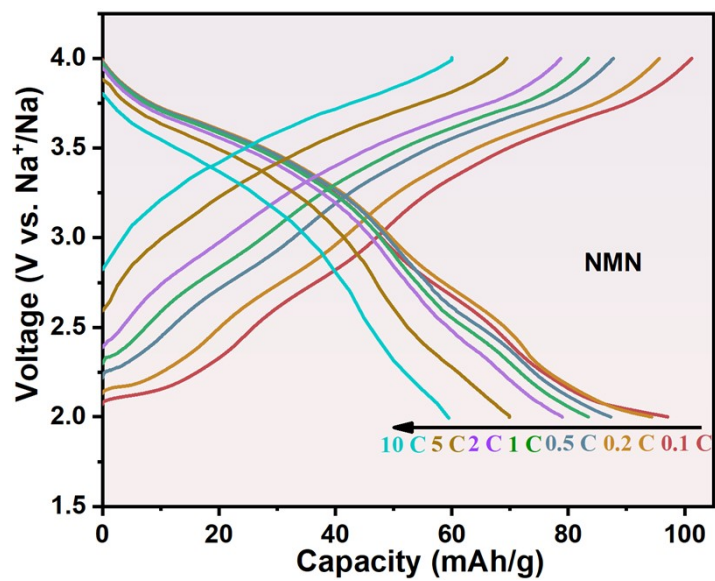


Figure S4. The first cycle charge/discharge profiles at various rates of NMN

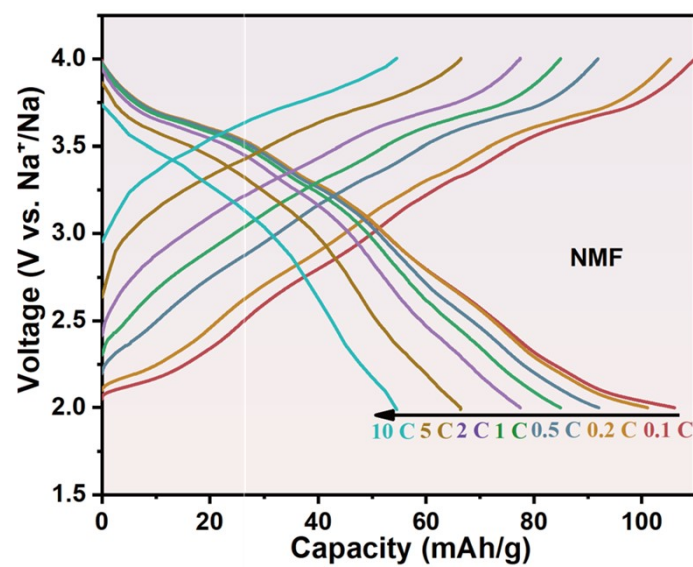


Figure S5. The first cycle charge/discharge profiles at various rates of NMF

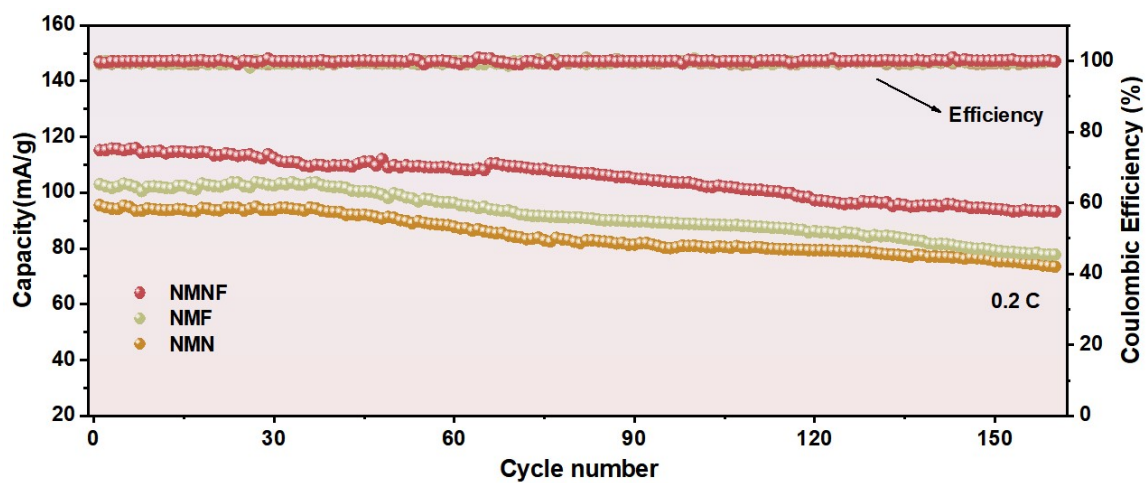


Figure S6. Cycling performance of NMNF, NMF and NMN cathode materials at 0.2C.

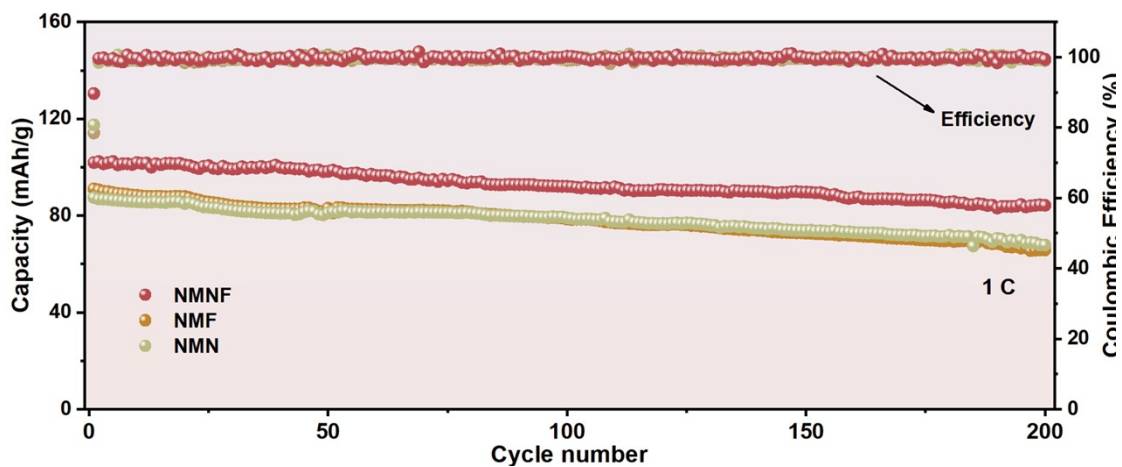


Figure S7. Cycling performance of NMNF, NMF and NMN cathode materials at 1C.

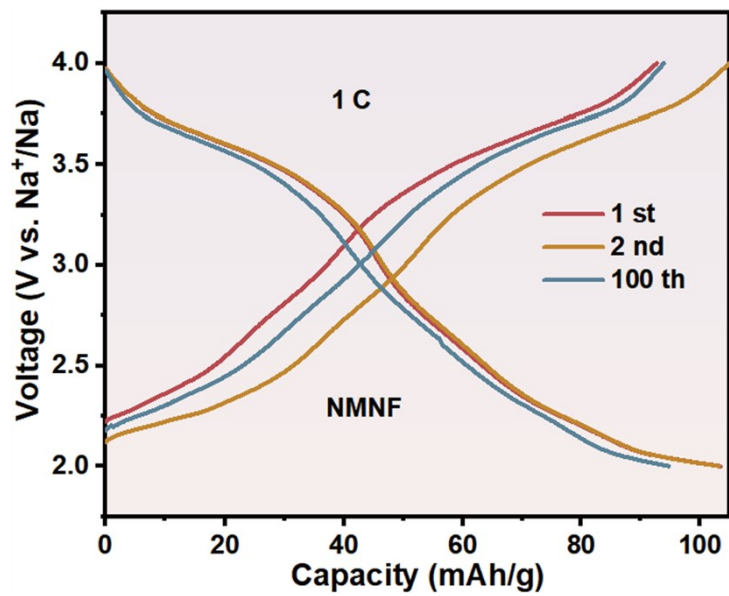


Figure S8. Charge-discharge curves of the NMNF cathode material at different cycles under 1C

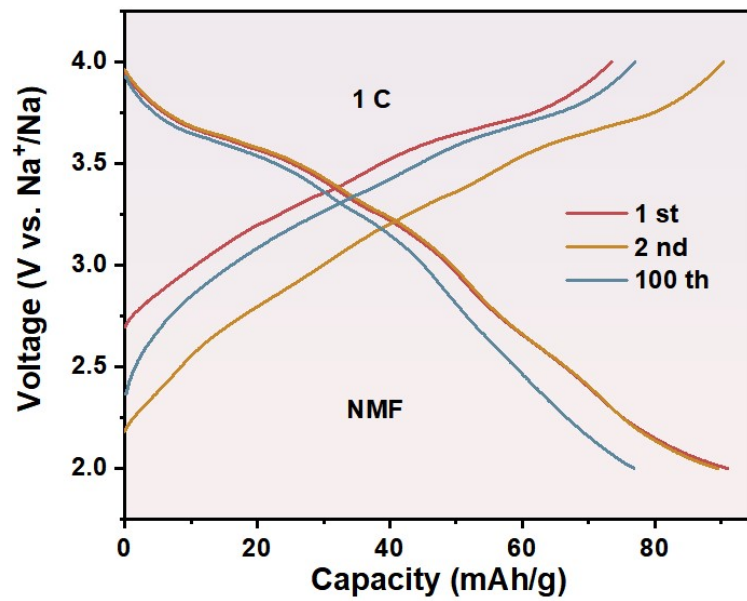


Figure S9. Charge-discharge curves of the NMF cathode material at different cycles under 1C

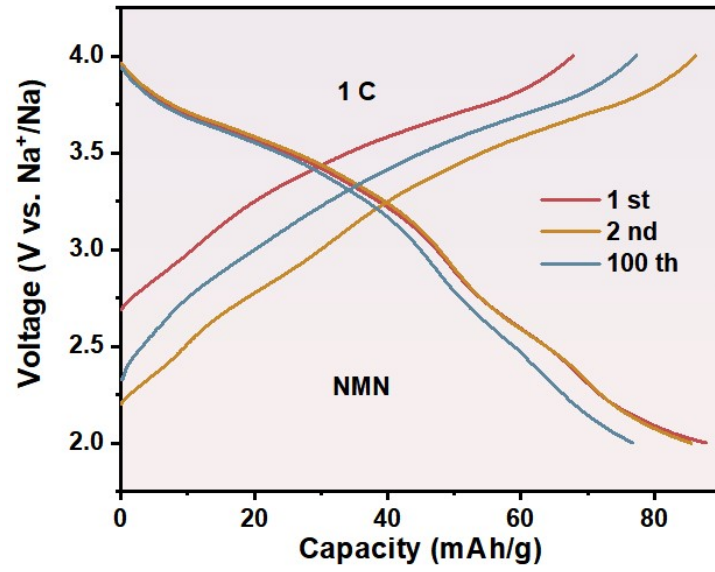


Figure S10. Charge-discharge curves of the NMN cathode material at different cycles under 1C

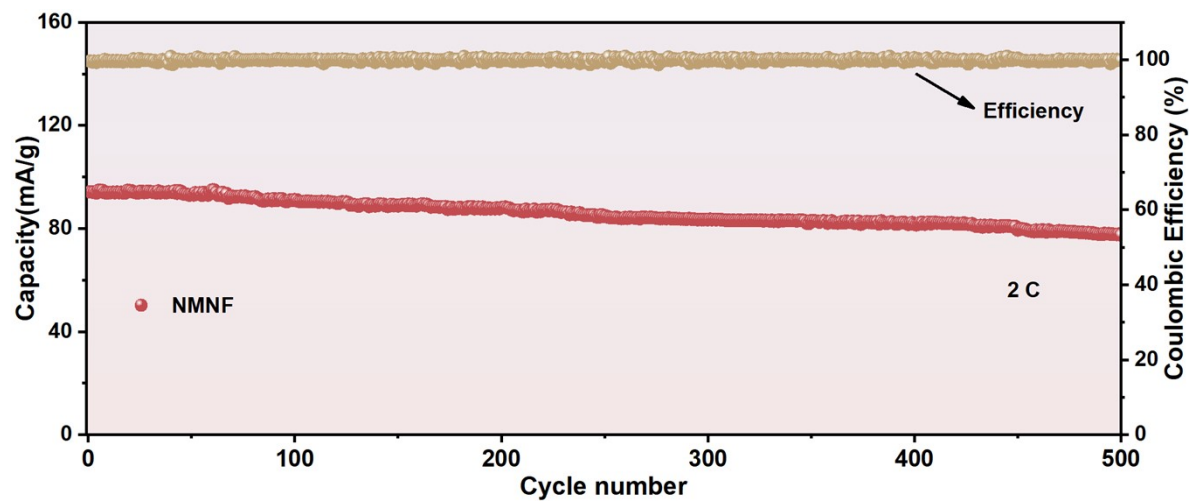


Figure S11. Cycling performance of NMNF cathode materials at 2C.

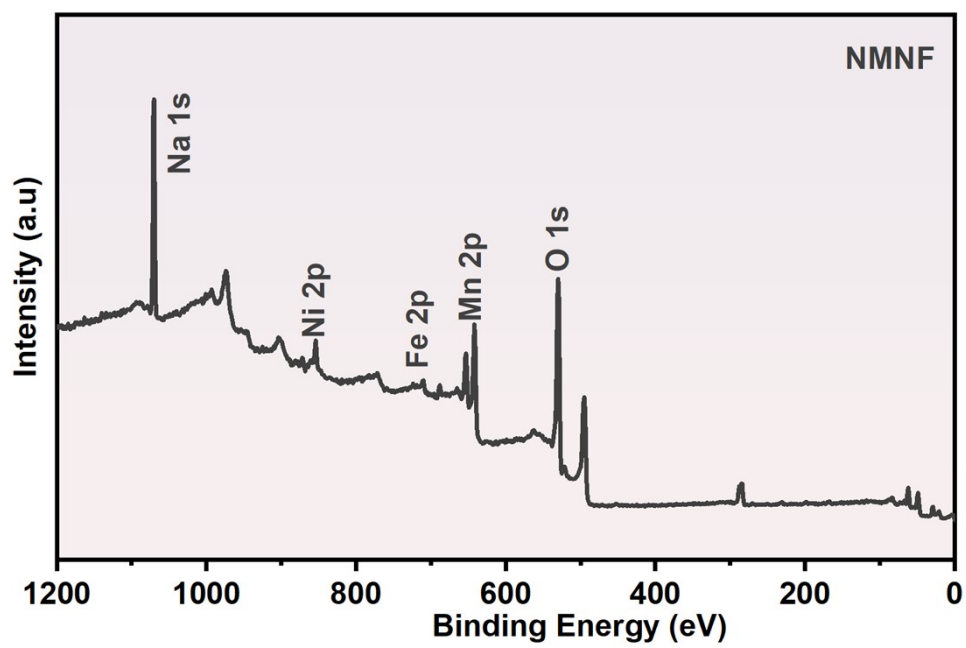


Figure S12. XPS full spectrum of NMNF.

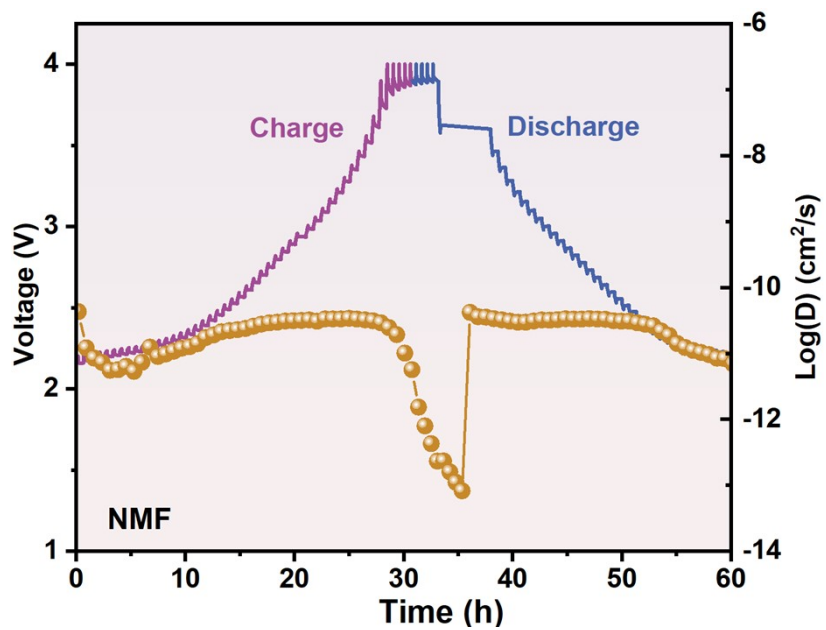


Figure S13. GITT curves of NMF cathode material in SIBs and corresponding sodium-ion diffusion coefficients  $D_{\text{Na}^+}$ .

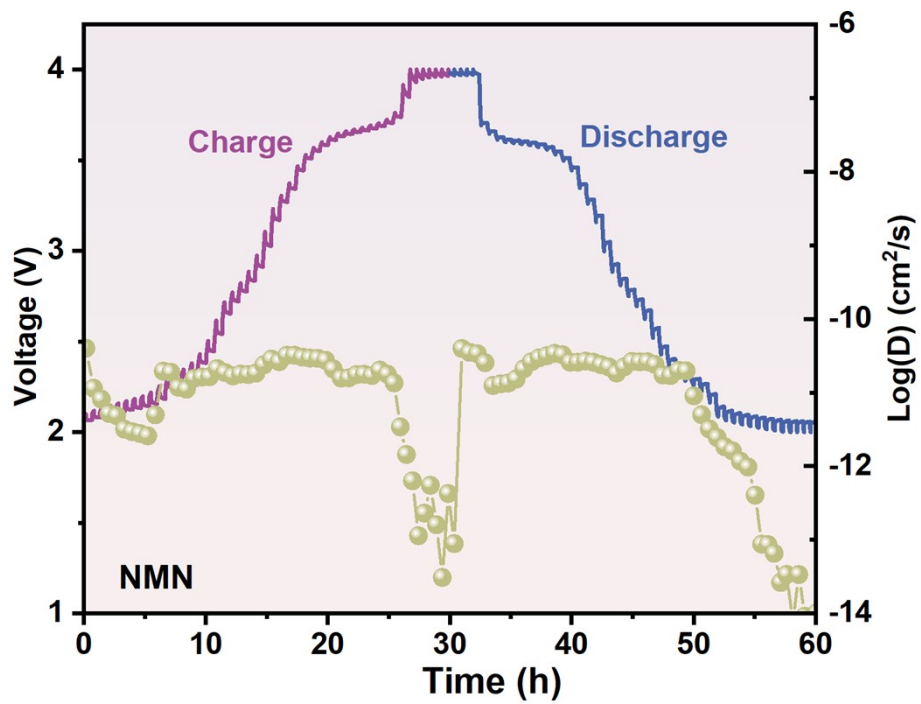


Figure S14. GITT curves of NMN cathode material in SIBs and corresponding sodium-ion diffusion coefficients  $D_{\text{Na}^+}$ .

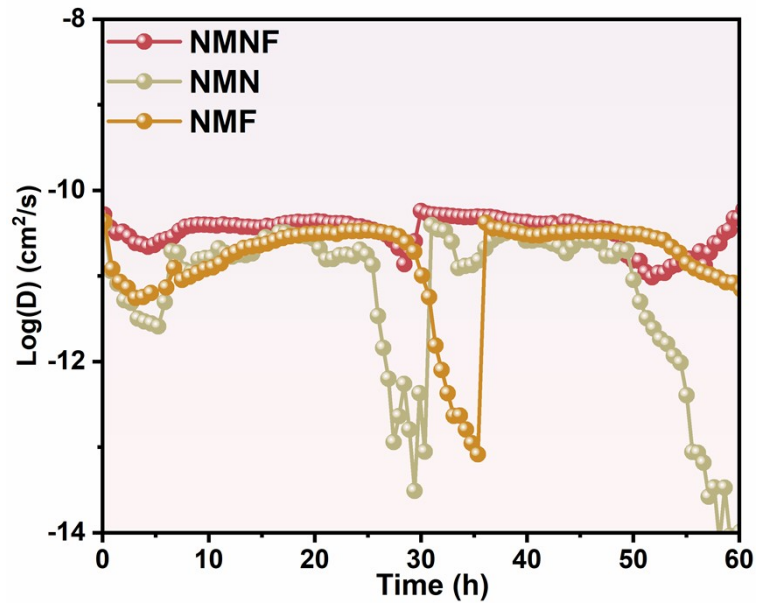


Figure S15. GITT curves of NMNF, NMN and NMF.

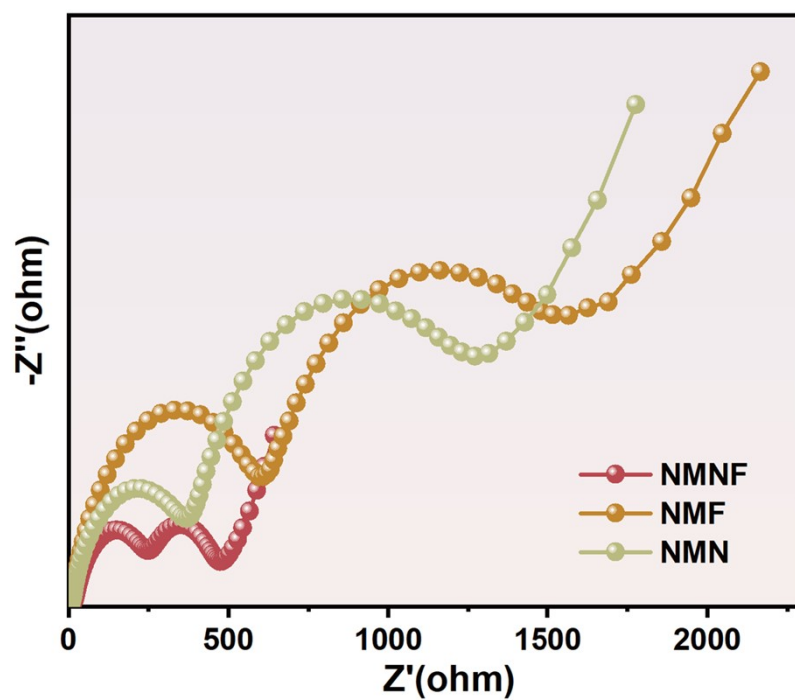


Figure S16. EIS plots of the NMNF, NMF and NMN electrodes.

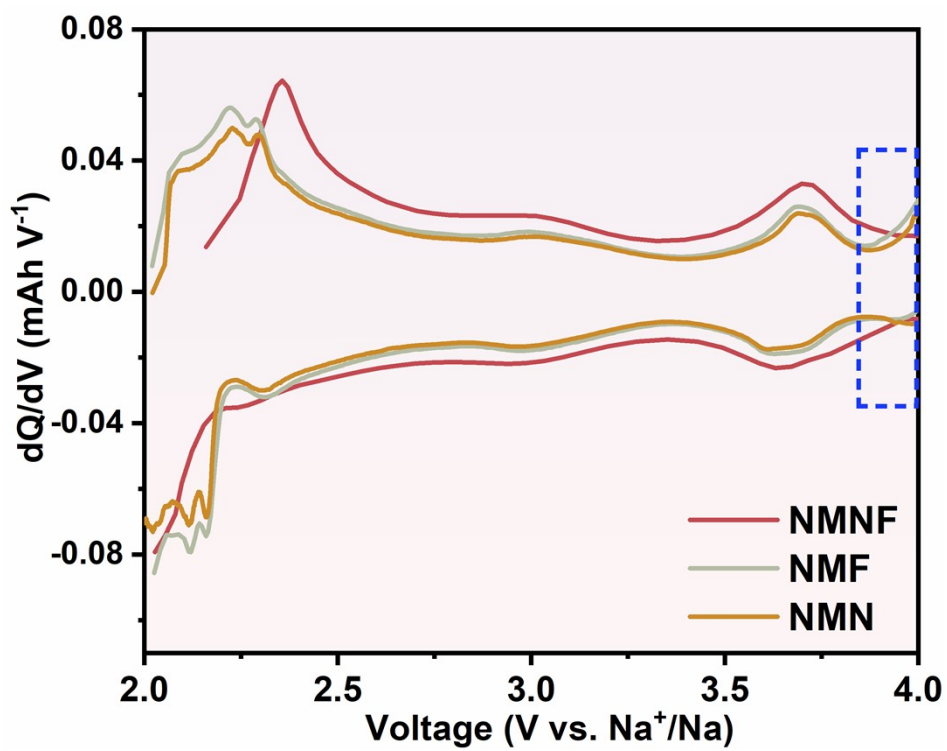


Figure S17.  $dQ/dV$  curves of NMNF, NMF and NMN.

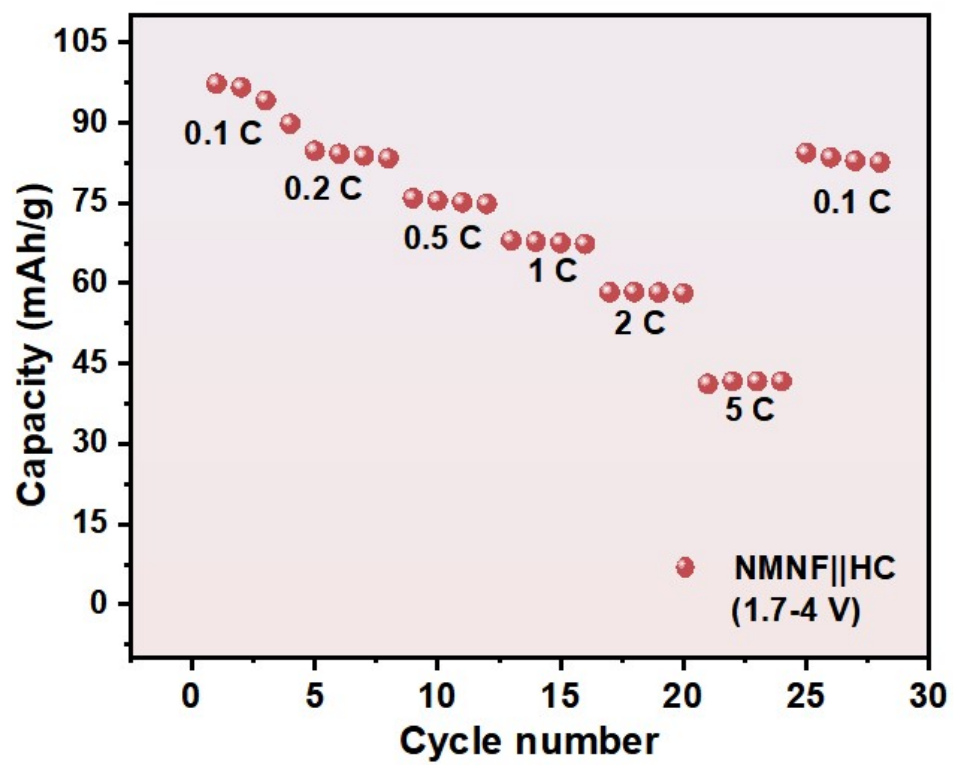


Figure S18. Rate performance of HC//NMNF full cell.

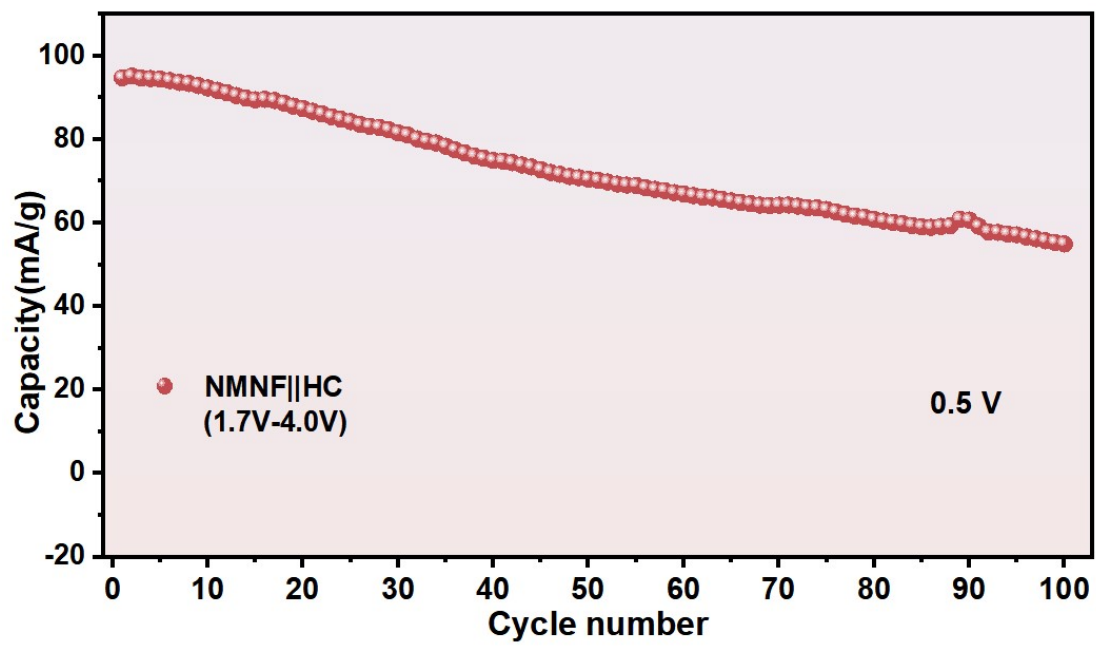


Figure S19. The long-cycling performance at 1C of HC//NMNF full cell.

Table S1. ICP-AES test results of NMNF, NMF and NMN samples

Samples	Measured atomic ratio			
	Na	Mn	Ni	Fe
NMNF	0.6666	0.7251	0.18466	0.0902
NMF	0.6679	0.8894	0	0.1063
NMN	0.6724	0.8023	0.2034	0